4ICEGE
Thessaloniki-GREECE 2007

4th International Conference on
Earthquake Geotechnical Engineering
June 25-28, 2007
Paper No. 1194

CYCLIC TRIAXIAL TESTING OF FULLY AND PARTIALLY SATURATED SOIL AT SILCHAR

Sanjay PAUL [1], Ashim Kanti DEY[2]

ABSTRACT

Silchar is located in the southern part of the state of Assam at North East India as shown in figure 1. It is seismically bounded by three faults and hence, earthquakes of magnitude 5.0 on Richter scale and above are very frequent in this part of Assam. Although, the soil at Silchar is predominantly clayey in nature, layers of silty sand are available near banks of Barak River and its tributaries. These layers contain water and are susceptible to liquefaction.

It is known that the nature and distribution of earthquake damage is strongly influenced by the dynamic properties of soil. The dynamic properties include variation of shear modulus and damping ratio at different strain levels caused by a dynamic load. A study has been made on determination of shear modulus and damping ratio of Silchar soil under different strain levels using cyclic triaxial testing apparatus. It is observed that, the shear modulus decreases and damping ratio increases with increase in strain level. Relationship of modulus reduction with effective confining pressure, relative density and strain levels have been obtained. The liquefaction analysis of Silchar soil has also been carried out.

Keywords: Shear modulus, Damping ratio, Strain level, Liquefaction, Cyclic triaxial testing apparatus

INTRODUCTION

The North-East India is located in seismic zone V, the highest zoning in the seismic zoning map of India and is experienced with frequent earthquakes; almost all of them are above magnitude 5.0 on Richter. Silchar is seismically bounded by Dauki fault in the north-west, Sitakunda – Teknaf fault in the south-west and Indo-Myanmar subduction zone in the east. Although, the soil at Silchar is predominantly clayey in nature, layers of silty sand are available near banks of Barak River and its tributaries. These layers contain water and are susceptible to liquefaction. Thin layers of saturated fine sand have also been found at various depths in the hilly areas which actuate sliding of overlying layers during earthquakes. For example, wide spread liquefaction occurred after Cachar earthquake in 1984 due to which many fissures and cracks were formed in the flat ground followed by sand and water ejection. A two minute tremor was felt in the early hours on 6th August, 1988 (Indo-Myanmar border earthquake, 1988) and large scale landslides, fissures, sand boiling were reported.

It is known that the nature and distribution of earthquake damage is strongly influenced by the dynamic properties of the soil. The dynamic properties include variation of shear modulus and damping ratio at different strain levels caused by an earthquake.

[1] Research Scholar, Department of Civil Engineering, National Institute of Technology, Silchar, India, Email: sanjaypaul_76@yahoo.com.
[2] Assistant Professor, Department of Civil Engineering, National Institute of Technology, Silchar, India, Email: akdey@nits.ac.in.

REVIEW OF LITERATURE

The nature and distribution of earthquake damage is strongly influenced by the response of soils to cyclic loading. Earthquake loading is random in nature and the random loading may be expressed as an algebraic sum of different cyclic loadings. This response is controlled in large part by the mechanical properties of the soil. For many important problems particularly those determined by wave propagation effects, only low levels of strain are induced in the soil. For other important problems, such as those involving the stability of masses of soil, large strains are induced in the soil. The behavior of soils subjected to dynamic loading is governed by what have come to be popularly known as dynamic soil properties.

Following types of dynamic loading may arise:
(a) Harmonic Loading; (b) Periodic Loading; (c) Random Loading; and (d) Transient Loading.

Since the earthquake loading is of random in nature, it becomes necessary to determine the equivalent number of significant uniform stress cycles of harmonic nature. The term 'equivalent' means that the effect of the irregular stress history on a given soil deposits should be same as the uniform stress cycles. Suppose τ_{max} is the maximum shear stress in an irregular stress-time history of an earthquake loading. Based on laboratory data, it has been found (with a reasonable degree of accuracy) that the average equivalent uniform shear stress τ_{av} is about 65 % of the maximum shear stress (After Das, 1983).

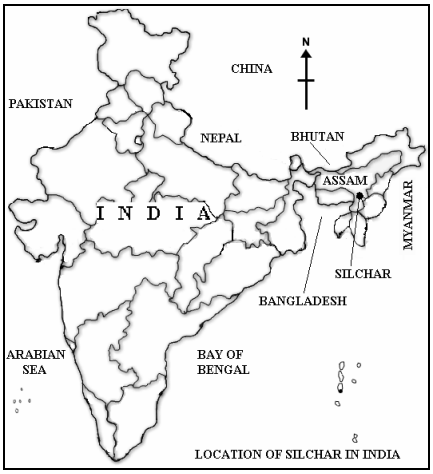

Figure 1. Location Map of Silchar

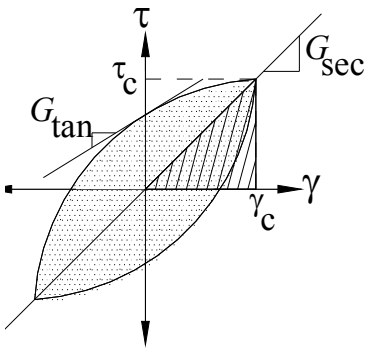

Figure 2. Secant shear modulus (G_{sec}) (After Kramer, 1996)

Dynamic Soil Properties

The major soil properties that need to be ascertained in soil dynamics and geotechnical earthquake engineering are:
(a) Shear strength against a permissible strain;
(b) Dynamic moduli, Young's modulus, shear modulus, bulk modulus, and constrained modulus;
(c) Poisson's ratio;
(d) Damping; and
(e) Liquefaction parameters: cyclic shearing stress ratio, cyclic deformation, and pore-pressure response.

Out of these, two important properties namely Shear modulus and Damping ratio are defined as follows:

Shear Modulus

Under a symmetrical cyclic loading, a typical soil element is subjected to stress-strain deformations in the form of a hysteresis loop as shown in figure 2. In general terms, two important characteristics of the shape of a hysteresis loop are its inclination and its breadth. The inclination of the loop depends on the stiffness of the soil, which can be described at any point during the loading process by the tangent shear modulus, G_{tan}. G_{tan} varies throughout a cycle of loading, but its average value over the entire loop can be approximately by the secant shear modulus

$$G_{sec} = \frac{\tau_c}{\gamma_c} \tag{1}$$

where τ_c and γ_c are the shear stress and shear strain amplitudes, respectively. Thus G_{sec} describes the general inclination of the hysteresis loop.

Damping Ratio

The breadth of the hysteresis loop as shown in figure 2 is related to the area, which as a measure of energy dissipation, can be conveniently described by the damping ratio

$$D = \frac{W_D}{4\pi W_S} = \frac{1}{2\pi}\frac{A_{loo\,p}}{G_{sec}\gamma_c^2} \tag{2}$$

where, W_D, W_S, A_{loop}, G_{sec} and γ_c are the dissipated energy, maximum strain energy, area of hysteresis loop, secant shear modulus and shear strain amplitude respectively.

Measurement of Dynamic Soil Properties

The measurement of dynamic soil properties is a critical task in the solution of geotechnical earthquake engineering problems. A wide variety of field techniques like Seismic Reflection test, Rayleigh Wave test, Seismic Cross-Hole test, Cone Penetration test, Pressuremeter test, etc. and laboratory tests like Resonant Column test, Ultrasonic Pulse test, Piezoelectric Bender Element test, Cyclic Triaxial test, etc. can be performed based on small or large strain of the soil specimen. There are a few model tests, namely, Shaking Table test, Centrifuge test, etc. The choice of a test depends upon initial stress conditions and anticipation of actual cyclic loading conditions at field.

Cyclic Shear Strain

The cyclic shear strain (γ) is defined as:

$$\gamma = (1+\mu).\varepsilon \tag{3}$$

where, μ = Poisson's ratio, which is taken as 0.4 for dry sands and 0.5 for saturated sands (RaviShankar et. al., 2005)

ε = Axial strain, which is expressed as a ratio between deformations of sample to its original length.

SOIL SAMPLING AND CHARACTERIZATION

Dry representative sand samples were collected from the different locations of Silchar town. It was observed that the physical characteristics of the samples are more or less uniform at all the places. Hence the samples were mixed in the laboratory to make a single specimen sample. Figure 3 shows a

typical grain size distribution of the specimen sample. Table 1 gives the other physical properties of the sample.

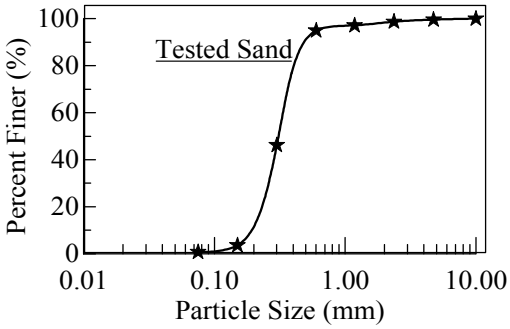

Figure 3. Grain Size Distribution of Specimen Soil

Table 2. Physical Properties of Sand Sample

G_s	2.648
e_{max}	0.822
e_{min}	0.570
D_{10} (mm)	0.19
D_{30} (mm)	0.26
D_{60} (mm)	0.35

TESTING EQUIPMENT USED IN THE PRESENT STUDY

A cyclic triaxial testing equipment (figures 4 and 5) has been used in the present study to measure the dynamic soil properties at high strain levels. The equipment is make of HEICO, India with different sensors, including a load cell to monitor the axial load, an LVDT to measure the vertical displacement, three transducers to detect the chamber pressure, pore pressure and volume change. The triaxial cell is built with low friction piston rod seal along with a 10 KN servo controlled submersible load cell. The loading system consists of a load frame and a hydraulic actuator capable of performing strain-controlled as well as stress-controlled tests (by servo hydraulic loaders) with wide range of frequency 0.1 Hz to 10 Hz.

The difference between the axial stress and the radial stress is called the deviator stress. In the cyclic triaxial test, the deviator stress is applied cyclically, either under stress-controlled conditions (typically by pneumatic or hydraulic loaders) or under strain-controlled conditions (by servo hydraulic or mechanical loaders). Cyclic triaxial tests are the most commonly performed with the radial stress held constant and the axial stress cycled at different frequencies.

In the present analysis, 38 mm diameter and 76 mm high samples were prepared and placed between top and bottom loading platens and surrounded by a thin rubber membrane. The specimen was subjected to vertical and horizontal stresses; hence the principal stresses were always vertical and horizontal.

SAMPLE PREPARATION

Dry sand specimens of above mentioned size with relative densities 40%, 50%, 60 % and 70% were prepared by pouring the pre weighted amount of dry sand through a funnel whose spout was placed at the bottom of the membrane lined split mould. The funnel was slowly raised along the axis of symmetry and the mould was filled with soil compacted in three layers to achieve the desired density. Tests were carried out on both saturated and unsaturated soil samples.

For full saturation, distilled water under a back pressure was used keeping the cell pressure little above the back pressure. After saturation Skempton's pore pressure parameter (Skempton,1954), $B = \Delta u/\Delta\sigma_c$, was checked, where, Δu = cyclic pressure and $\Delta\sigma_c$ = rise in cell pressure. For all the tests, under full saturated conditions, B value was kept as 0.95. After the saturation, the sand specimens were consolidated under a pre-defined isotropic stress condition.

For partial saturation of the soil, the samples were saturated to different degree of saturation. This was done by pouring a measured volume of water through a standpipe into the sand samples Some idle time was allowed for free movement of water throughout the sample.

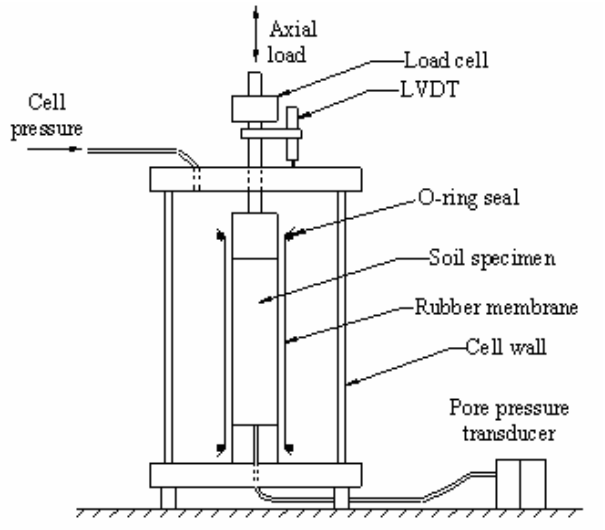

Figure 4. Typical Triaxial Apparatus (After Kramer, 1996)

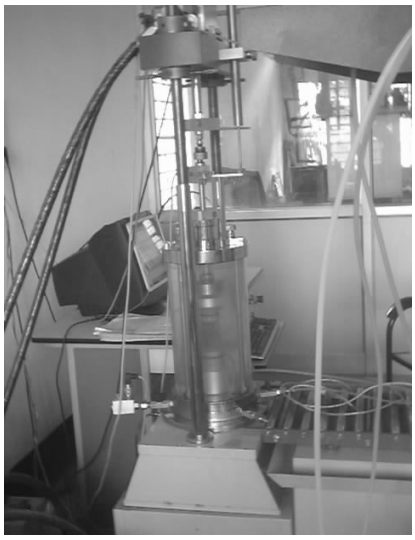

Figure 5. Cyclic Triaxial Testing Machine

CYCLIC LOADING AND DATA ACQUISITION

Cyclic loading in the vertical direction was applied directly on the soil samples using strain-controlled method. The tests were carried out as per ASTM (1996) with different strain, relative densities, confining pressures and degree of saturations at a sinusoidal harmonic loading of frequency 0.1 Hz and 1.0 Hz. For fully saturated sand samples the tests were conducted with different shear strains (γ) from 1.974 % to 5.921 % at different relative densities from 40 % to 70 % (f = 1.0 Hz). For unsaturated sand samples the tests were conducted for different strain amplitudes (γ) from 0.54 % to 4.73 % at different relative densities from 40 % to 80 % (f = 0.1 Hz) at different degrees of saturation.

RESULTS AND DISCUSSION

Evaluation of Dynamic Properties and Liquefaction Potential of Fully Saturated Soil

Figures 6 shows the relationship between dynamic properties versus shear strain for saturated sand samples at relative densities of 40 %, 50 % 60 % and 70 % under a confining pressure of 100 kPa and at a frequency of 1 Hz. It is evident form the figures that, shear modulus reduces and damping ratio increases for any relative density with the increase of shear strain. At a particular shear strain the G value remains higher for a denser sample and the D value remains higher for a loose sample when confining pressure remains constant..

Figure 7 shows the relationship between G and γ and D and γ respectively for saturated sand samples at confining pressures of 50 kPa, 100 kPa, 150 kPa and 200 kPa under a relative density of 60 % and at a frequency of 1 Hz. It is evident form the figures that, shear modulus value reduces and the damping value increases with the increase of shear strain. At a particular shear strain the G value remains higher for higher confining pressure and the D value remains higher for lower confining pressure when relative density of sample remains constant.

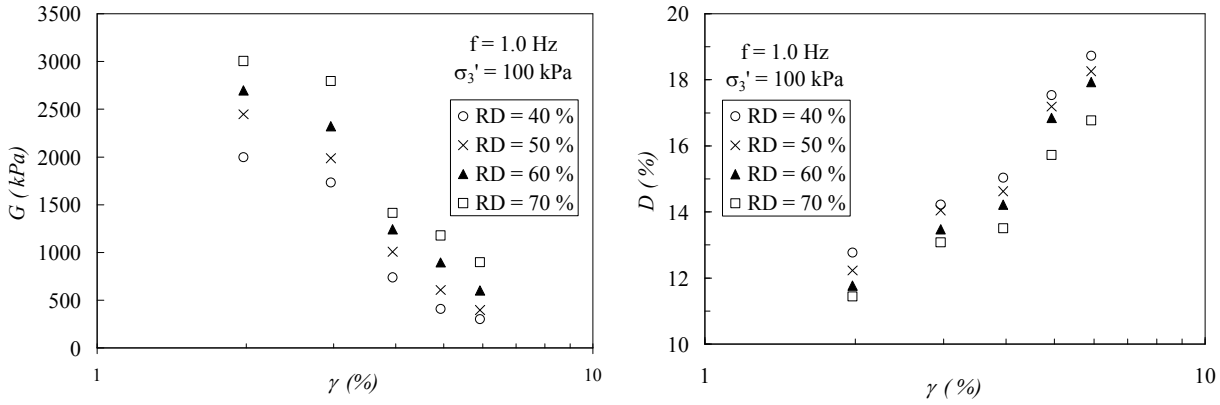

Figure 6. Variation of (a) Shear Modulus (*G*) and (b) Damping Ratio (*D*) with Shear Strain (γ) for a constant confining pressure (σ_3' = 100 kPa)

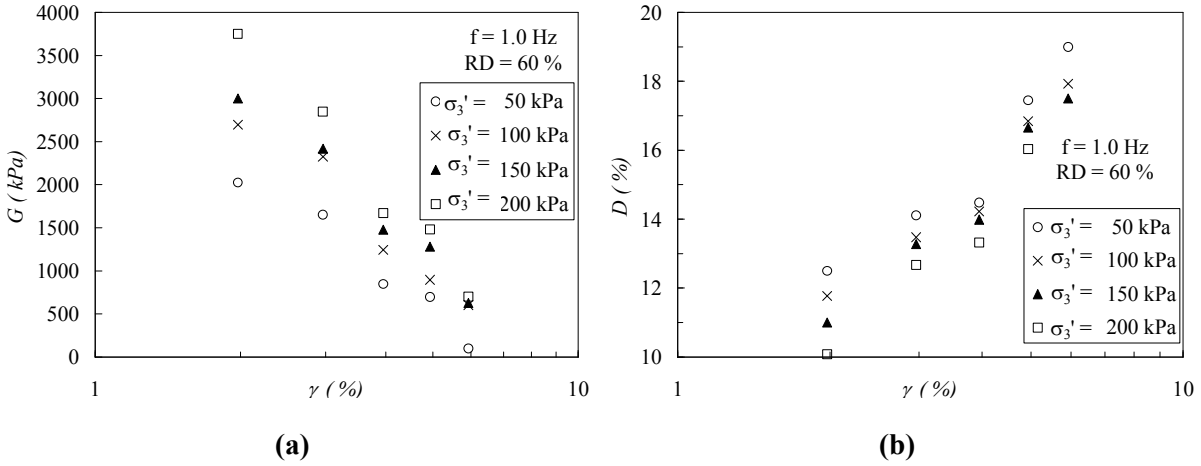

Figure 7. Variation of (a) Shear Modulus (*G*) and (b) Damping Ratio (*D*) with Shear Strain (γ) for a constant relative density (RD = 60 %)

Figure 8 shows the variation of deviator stress (σ_d), axial strain (ε) and pore pressure ratio (r_u) with time for the sand at a strain-controlled cyclic test. It is evident from the figure that the pore water pressure builds up steadily during application of cyclic shear strain and eventually approaches a value equal to the initial confining pressure. For the sample tested at 40 % of RD and 100 kPa confining pressure, the cyclic pore pressure ratio becomes 100 % after 30 cycles at 2.961 % shear strain, which is known as liquefaction. It can be seen that the increase in pore water pressure results in a corresponding decrease in the deviator stress, which finally becomes constant. Such a state of the specimen is recognized as 'liquefaction' which is a state of softening produced suddenly with complete loss of shear strength or stiffness.

A typical hysteresis loop during a cyclic triaxial test in the present study is as shown in figure 9. It is observed in the figure that, as the cyclic load is applied the area of hysteresis loop reduces due to loss of shear strength of the soil sample.

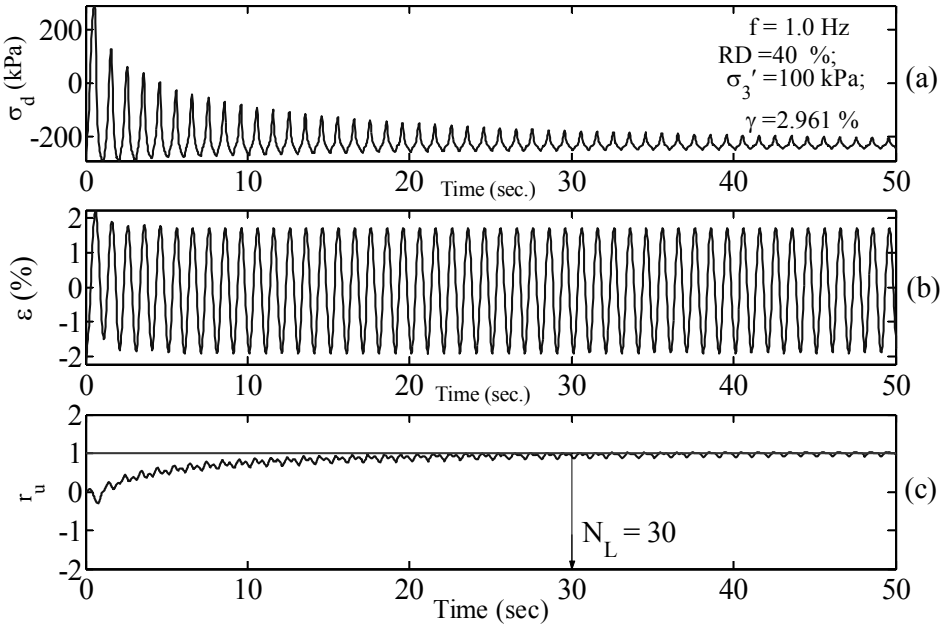

Figure 8. Variation of (a) deviator stress, (b)axial strain and (c) pore pressure ratio with time

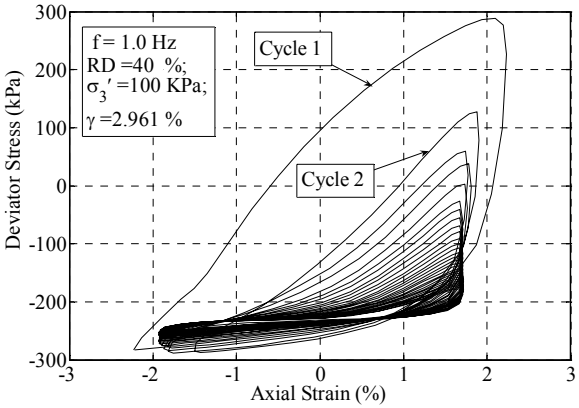

Figure 9. Typical Hysteresis Loops

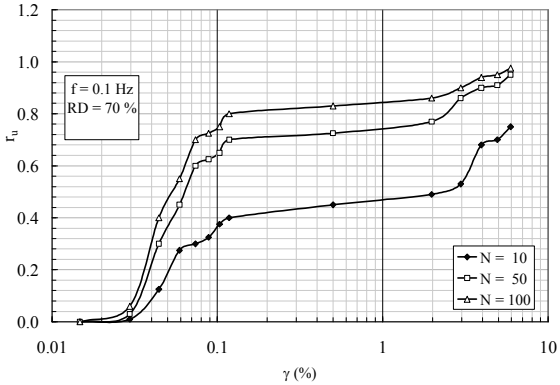

Figure 10. Typical Hysteresis Loops

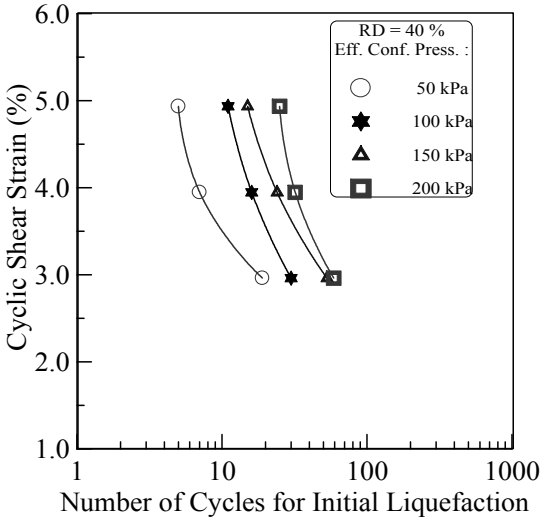

Figure 11. Cyclic Resistance Curve for constant Relative density

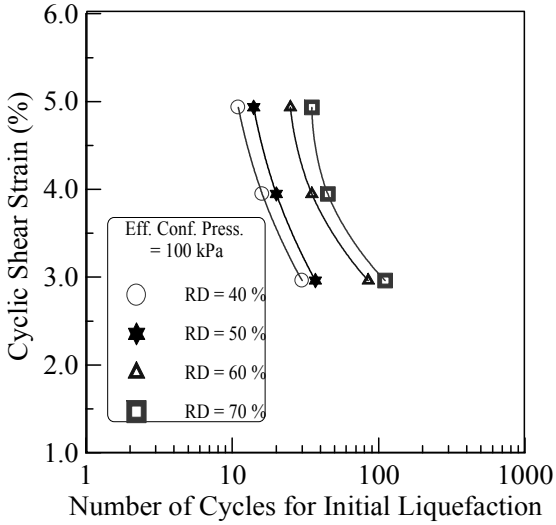

Figure 12. Cyclic Resistance Curve for constant Confining Pressure

Evaluation of liquefaction potential can be done either by cyclic stress method or cyclic strain method. In strain-controlled tests, there is a predictable correlation between cyclic shear strain, number of cycles, and pore-water pressure buildup; this correlation is much less sensitive to factors, such as relative density and fabric than comparable results obtained from stress-controlled tests (Ladd et.al., 1989). In the present analysis, strain controlled tests were conducted and a threshold shear strain of approximately 0.015 % has been obtained. Figure 10 shows the threshold shear strain value for a test sample.

Figures 11 and 12 represent the cyclic resistance in terms of cyclic shear strain vs. number of cycles for initial liquefaction for constant confining pressure and constant relative density respectively.

Evaluation of Dynamic Properties of Partially Saturated Soil

Typical variation of deviator stress, axial strain and pore pressure rise against time is shown in figure 13. The strain levels were increased after every 10 cycles. It can be seen that pore pressure increases gradually and then decreases suddenly. Similar results were obtained at all confining pressures and relative densities of sand samples.

Variation of pore pressure with number of cycles for different degree of saturations (S_r) is shown in figure 14. It can be seen that for all the cases, except S_r = 100 % pore pressure builds up initially, reaches a maximum value and then drops suddenly. It was observed that most of the unsaturated sand samples failed in shear along a diagonal plane.

Typical variation of shear modulus and damping ratio with shear strain at different confining pressures is shown in figure 15. It is observed that irrespective of confining pressure, shear modulus decreases and damping ratio increases with strain.

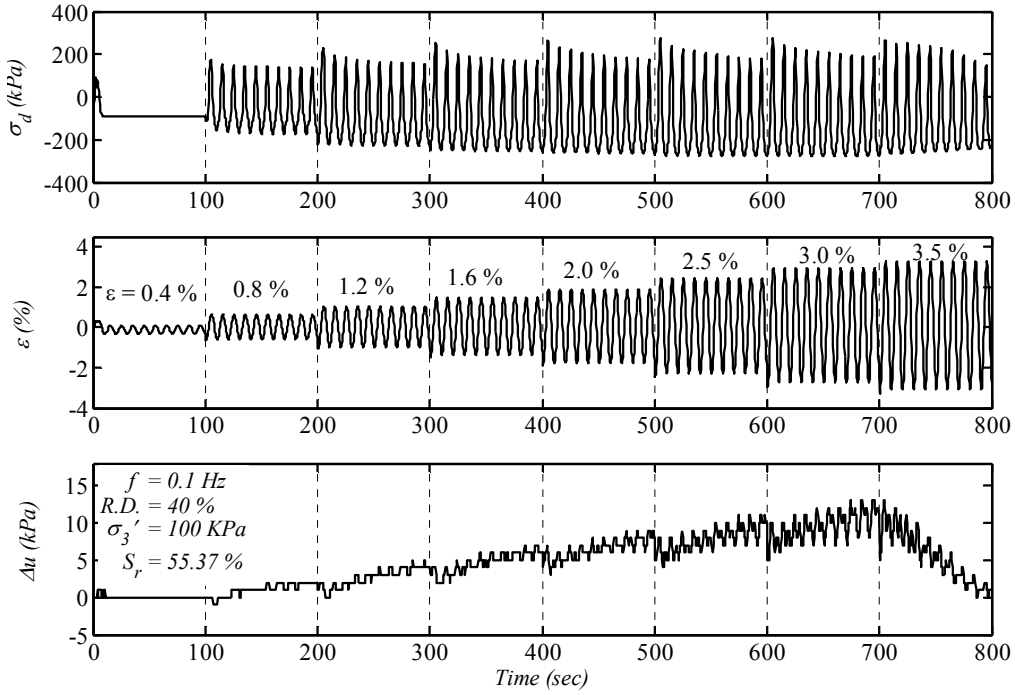

Figure 13. Typical results of a strain-controlled cyclic triaxial test

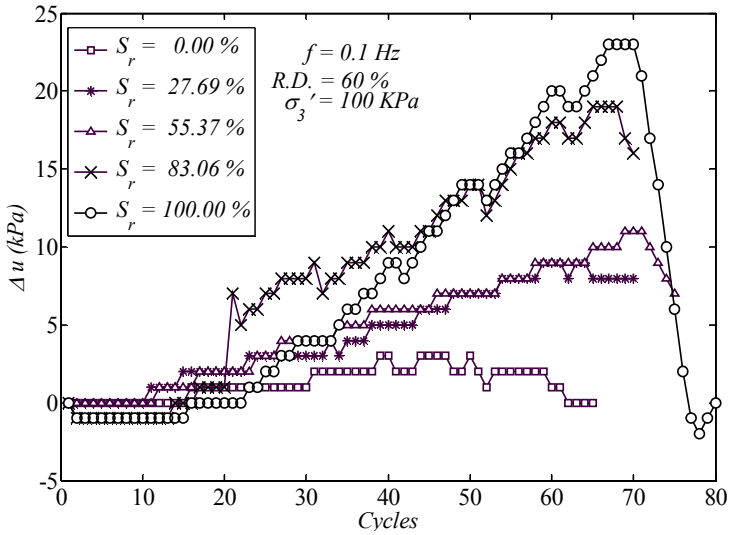

Figure 14. Change in pore pressure (Δu) with number of cycles for different degree of saturations (S_r)

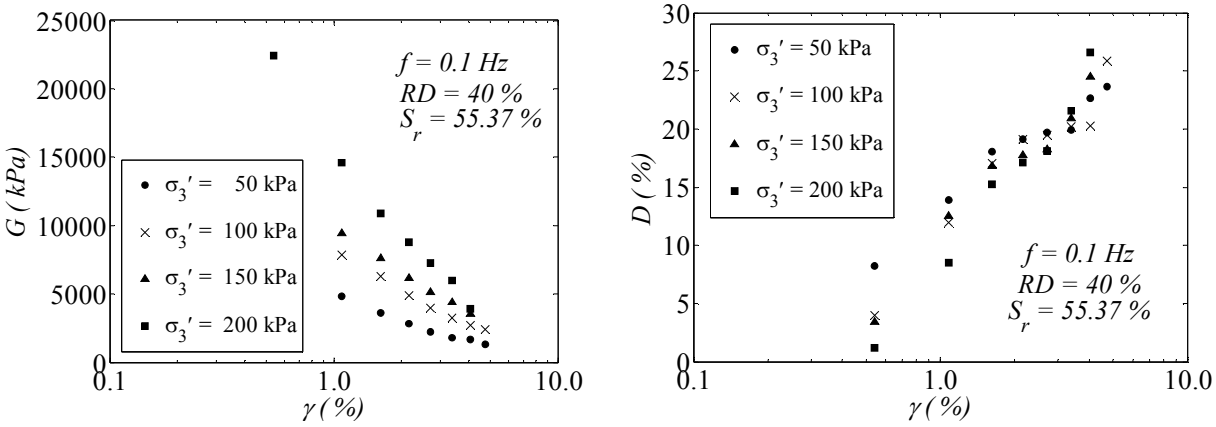

(a) **(b)**

Figure 15. Variation of (a) shear modulus (G) and (b) damping ratio (D) with shear strain (γ) at different effective confining pressures

Variation of shear modulus with different degree of saturation is shown in figure 16 (a). It can be seen that with increase in degree of saturation shear modulus increases, reaches a maximum value at an optimum degree of saturation and then decreases sharply. This optimum value of degree of saturation corresponding to maximum value of shear modulus may arise due to the following factors :
(a) Development of micro fracture of the soil samples during drying (Marinho et. al. 1995) due possibly to abrupt changes in water content, or
(b) Reduction of the capillary effects during shear deformation, which involves particle displacement and particle rotation (Mendoza and Colmenares, 2006).

Variation of damping ratio with different degree of saturation is shown in figure 16 (b). Damping ratio reduces with the increase of degree of saturation. Figure 17 shows the comparison of hysteresis loops of sand samples at different degree of saturations. From the figure it is observed that, as the degree of saturation increases the hysteresis loop area reduces. It represents that damping ratio reduces with the increase of degree of saturations, which is again clear from figure 16 (b).

Figure 18 shows the p'–q plot for different S_r values,

where,

$$p' = \frac{(\sigma_1' + \sigma_3')}{2} \tag{4}$$

$$q = \frac{(\sigma_1 - \sigma_3)}{2} \tag{5}$$

It is seen that, change in pore pressure during cyclic load application is not constant for loading and unloading operations. This change is more prominent for higher degree of saturation.

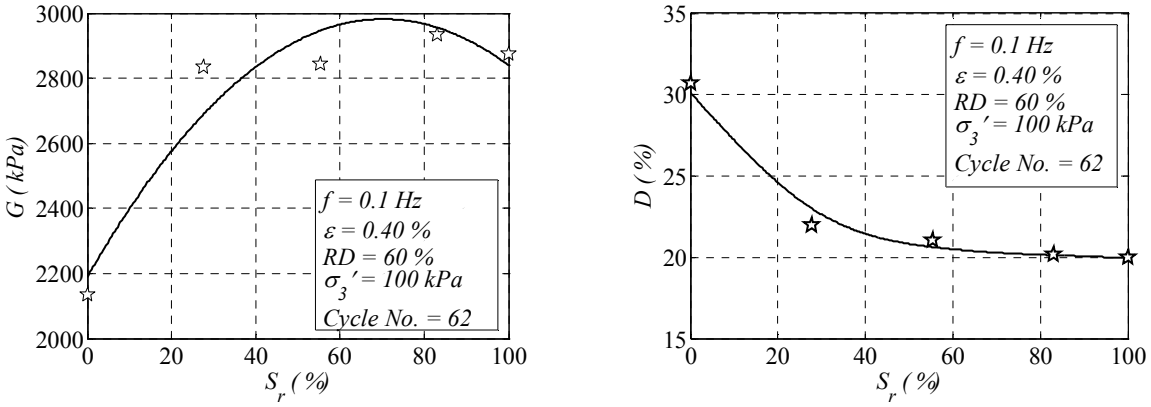

(a) **(b)**

Figure 16. Variation of (a) shear modulus (*G*), (b) damping ratio (*D*) with S_r

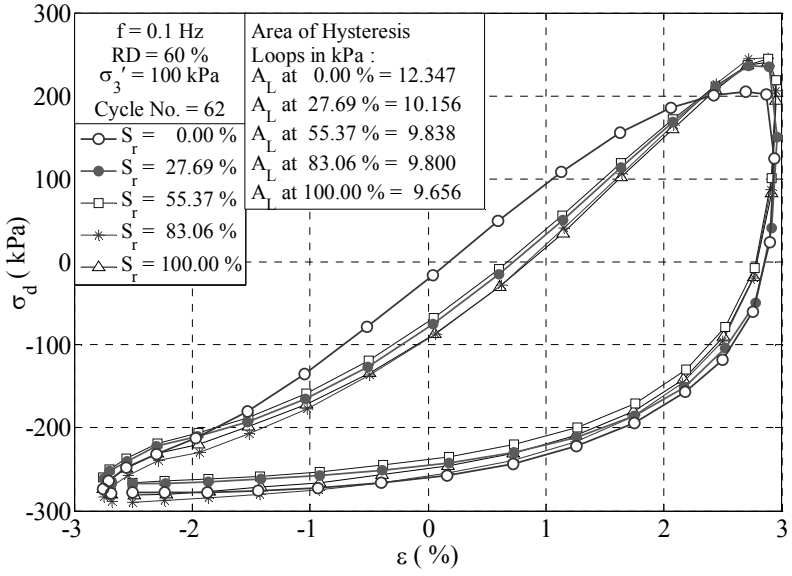

Figure 17. Comparison of hysteresis loops at different degree of saturations

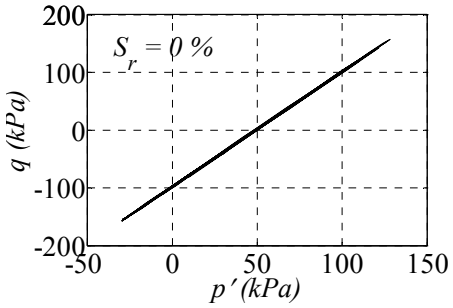

(a) S_r = 0.00 %

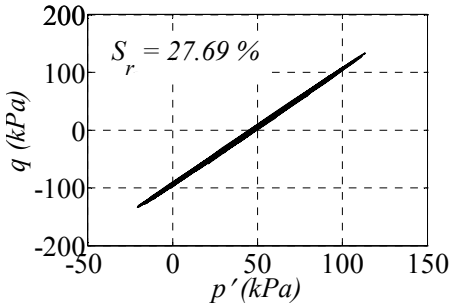

(b) S_r = 27.69 %

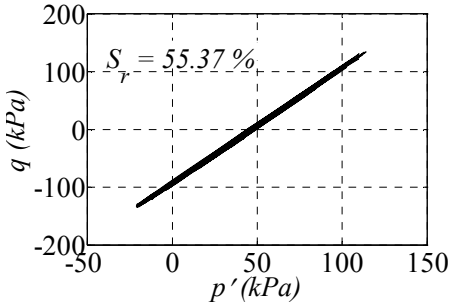

(c) S_r = 55.37 %

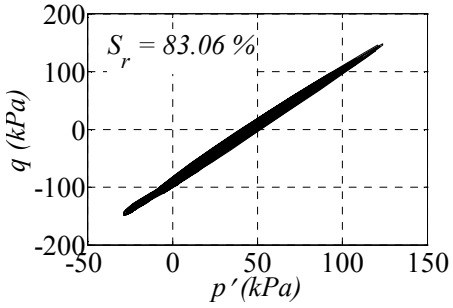

(d) S_r = 83.06 %

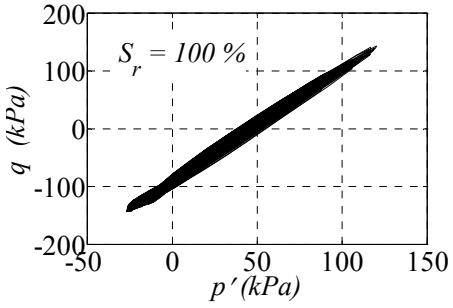

(e) S_r = 100.00 %

Figure 18. Variation of stress-path for different degree of saturations (a) – (e) at f = 0.1 Hz, R.D. = 60 % , σ_3= 100 kPa

CONCLUSIONS

Following conclusions can be drawn from the present study on local soil :

For full saturated condition –
Under full saturation, local soil behaves similar to already reported behavior of soil like reduction of shear modulus with increase in shear strain and increase in damping ratio with increase in shear strain. However, following additional points were noted :

(a) At a particular shear strain the *G* value remains higher for a denser sample and the *D* value remains higher for a loose sample when confining pressure remains constant. Again at a particular shear strain the *G* value remains higher for higher confining pressure and the *D* value remains higher for lower confining pressure when relative density of sample remains constant.

(b) When a cyclic load is applied on the soil, pore water pressure builds up steadily and reaches initially applied confining pressure depending on the magnitude of cyclic shear strain as well as on the density of the soil.

(c) The amplitude of cyclic shear strain governs the liquefaction resistance of a soil characterized by the cyclic strain approach. A threshold strain of approximately 0.015 % is obtained in the present analysis.

For unsaturated condition –

(a) With increase in number of cycles, pore pressure increases gradually and then decreases suddenly. The samples failed in shear along a diagonal plane.

(b) Irrespective of confining pressure, shear modulus decreases and damping ratio increases with strain.

(c) The rise of pore pressure with number of cycles is more for low relative density.

(d) With the increase in degree of saturation, the shear modulus of soil increases, reaches a optimum value and then decreases at a particular strain level.

(e) Damping ratio reduces with the increase in degree of saturation, as the area of hysteresis loop increases with the increase of the degree of saturation at a particular strain level.

(f) The change in pore pressure during cyclic load application is not constant for loading and unloading operations. This change is more prominent for higher degree of saturation.

REFERENCES

ASTM Designation: D 3999-91 (Reproduced 2003). "Standard Test Methods for the Determination of the Modulus and Damping Properties of Soils using the Cyclic Triaxial Apparatus," Annual Book of ASTM Standards, 1996.

ASTM Designation: D 5311-92 (Reproduced 2004). "Standard Test Methods for Load Controlled Cyclic Triaxial Strength of Soil," Annual Book of ASTM Standards, 1996.

Das, B.M. "Fundamentals of Soil Dynamics," Elsevier Publications, New York, 1983.

Ladd, R.S., Dobry, R., Dutko, P.,Yokel, F.Y. and Chung R.M. "Pore-Water Pressure Buildup in Clean Sands Because of Cyclic Straining," Geotechnical Testing Journal, Vol. 12, Issue 1, 1989.

HEICO. "Manual for Cyclic / Static Triaxial test System," (Conforming to ASTM D-5311-92).

Kramer, S.L. "Geotechnical Earthquake Engineering," Prentice Hall, New Jersey, l996.

Marinho, F., Chandler, R. and Crilly, M. "Stiffness Measurements on an Unsaturated High Plasticity Clay Using Bender Elements." Proceeding 1st International Conference on Unsaturated Soils. Vol. 2, pp. 535-539, 1995.

Mendoza, C.E. and Colmenares, J.E. "Influence of the Suction on the Stiffness at Very Small Strains." Proceeding 4th International Conference on Unsaturated Soils, pp. 529-540, 2006.

Prakash, S. "Soil Dynamics." McGraw-Hill Book Company, 1981.

RaviShankar, B., Sitharam, T.G. and Govinda Raju, L. "Dynamic Properties of Ahmedabad Sands at Large Strains," Proceedings, Indian Geotechnical Conference-2005, Ahmedabad, INDIA, pp. 369-372, 2005.

Skempton, A.W. "The Pore Pressure Coefficients A & B," Geotechnique, 4, pp. 143-147, 1954.